

INITIATING THE NEWTONIAN GRAVITATIONAL N -BODY SPHERICAL SIMPLIFICATION ALGORITHM ON THE INOPIN HOLOGRAPHIC RING TOPOLOGY

Nathan O. Schmidt
Department of Mathematics
Boise State University
1910 University Drive
Boise, Idaho 83725, USA
nathanschmidt@u.boisestate.edu

August 3, 2014

Abstract

We propose a *preliminary* algorithm which is designed to reduce aspects of the n -body problem to a 2-body problem for holographic principle compliance. The objective is to share an alternative view-point on the n -body problem to try and generate a simpler solution in the future. The algorithm operates 2D and 3D data structures to initiate the encoding of the chaotic dynamical system equipped with modified superfluid order parameter fields in both 3D and 4D versions of the Inopin holographic ring (IHR) topology. For the algorithm, we arbitrarily select one point-mass to be the origin and, from that reference frame, we subsequently engage a series of instructions to consolidate the residual $(n - 1)$ -bodies to the IHR. Through a step-by-step example, we demonstrate that the algorithm yields “IHR effective” (IHRE) net quantities that enable us to hypothetically define an IHRE potential, kinetic, and Lagrangian.

Keywords: Newtonian mechanics; Relativistic mechanics; Gravitation; Holographic principle; Inopin holographic ring; Geometry and topology; Chaos; Spontaneous symmetry breaking; Superfluid order parameters.

1 Introduction

The n -body problem is the ancient problem of predicting the motion of a group of celestial objects that gravitationally interact with each other [1, 2]. Solving this problem has been motivated by the need to understand the motion of, for example, planets, stars, and black holes. Its first complete mathematical formulation appeared in Isaac Newton's Principia [1, 2]. Since gravity is responsible for the motion of planets and stars, Newton had to express gravitational interactions in terms of differential equations [1, 2]. In the Principia [1, 2], Newton proved that a *spherically-symmetric* body can be modeled as a point-mass. Interestingly, quantized particles may also be modeled as point-masses [3, 4, 5, 6], which seems to indicate that a solution to the n -body problem may be applied to a future unified theory of quantum gravity. To date, the 2-body problem has been completely solved, but only certain solutions exist for the 3-body problem [7].

Over a century ago, Poincaré's work on the *restricted* version of the 3-body problem formed the foundation of deterministic chaos theory [7]. Chaos theory studies the behavior of dynamical systems that are highly sensitive to initial conditions [8, 9]. In a chaotic dynamical system, minuscule differences in initial conditions yield widely diverging outcomes, thereby generally rendering long-term predictions impossible [8, 9]. Chaos is abundant in nature [9, 10, 11], and such complex, non-linear systems are widely studied in mathematics [12, 13, 14], physics [15, 16, 17], gravitation and cosmology [18, 19], astrophysics [20, 21], chemistry [22, 23, 24], biology [25, 26, 27, 28, 29, 30, 31, 32], neuro-science [33, 34, 35], medicine [36, 37], computation [38, 39, 40], cryptology [41, 42, 43], economics [44, 45], and warfare [46, 47, 48]. Chaos theory has significantly enhanced our general scientific comprehension of a wide range of phenomena, from structural dynamics to turbulence [8, 9, 46, 49] which applies to, for example, aquatic ecosystems [50], weather [51], black holes [15], the cosmic microwave background [19], galaxy distributions [20, 21], population biology [25], viruses and pathogens [26], cancers and genetics [27, 52], military strategy [46, 47, 48], volcanoes [53], earthquakes [54, 55], and the global stock market [44]. Moreover, we note that *fractals are the language of chaos theory* [56, 57, 58], where fractals are clearly everywhere in nature [12, 59] including, for example, the allometric scaling laws in biology [28, 29, 30, 31, 32]. The plethora of

well-documented scientific evidence for naturally-recurring n -body problems fundamentally conveys the significance pertaining to this mode of research. Thus, it is imperative to investigate such phenomenon from diverse perspectives and attack these problems from multiple directions.

In this introductory paper, we propose the *Newtonian Gravitational n -Body Spherical Simplification Algorithm* (NGNBSSA), which attempts to simplify the apparent complexity of the *unrestricted* version of the ($n > 2$)-body problem to that of a 2-body problem, for which the $n = 2$ solution *does exist*; the objective is to share an alternative view-point on the n -body problem with a spherically-symmetric topology to try and generate a solution (or partial solution) in the future. The NGNBSSA is a well-defined procedure of instructions that engages the 2D/complex and 3D/triplex data structure framework of [60] to encode 3D and 4D versions of the (spherically-symmetric) IHR topology [61] equipped with modified superfluid order parameter fields [62] for holographic principle compliance [63].

In Section 2, we prepare for our systematic n -body attack by assembling the requisite data structures for characterizing the chaotic gravitational system state space. First, in Section 2.1, we devise the 2D data structures for encoding 2D locations and 2D features in the 3D IHR topology of [60, 61]. Subsequently, in Section 2.2, we contrive the 3D data structures for encoding 3D locations and 3D features in the 4D IHR topology of [60].

Next, in Section 3, we present the NGNBSSA via a step-by-step example of instructions and illustrations. Thereafter, Section 3.1 demonstrates how the NGNBSSA systematically operates in the 3D IHR topology with the complex encoding framework [60, 61], while Section 3.2 explains how to adjust the NGNBSSA so it can also function in the 4D IHR topology with the triplex encoding framework [60]. In both scenarios, we use the results to define an IHRE potential, kinetic, and Lagrangian that aims to intertwine mechanics from Newton and Einstein.

Finally, the paper terminates with the conclusive discussion and future outlook of Section 4, followed by the brief concessions of Section 5.

2 Data structures

In this section, we prepare for the NGNBSSA by assembling the n -body chaotic gravitational system state space for encoding locations and features

in the 3D *and* 4D IHR topologies [60, 61].

2.1 2D structures in the 3D IHR topology

To encode 2D locations, we identify the Riemann surface X as the *2D Position-Point State Space* (2D-PPSS) [60, 61]. Thus, we define

$$P_X \subset X = \{\vec{x}_1, \vec{x}_2, \dots, \vec{x}_n\} \quad (1)$$

as the ordered set of spherically-symmetric point-particles of cardinality $n = |P_X|$ with the corresponding generalized *2D Riemannian-coordinates* [60, 61]

$$\begin{aligned} 1 : \vec{x}_1 &= (\vec{x}_1) = (|\vec{x}_1|, \langle \vec{x}_1 \rangle)_P = (\vec{x}_{1\mathbb{R}}, \vec{x}_{1\mathbb{I}})_C \\ 2 : \vec{x}_2 &= (\vec{x}_2) = (|\vec{x}_2|, \langle \vec{x}_2 \rangle)_P = (\vec{x}_{2\mathbb{R}}, \vec{x}_{2\mathbb{I}})_C \\ &\dots \\ n : \vec{x}_n &= (\vec{x}_n) = (|\vec{x}_n|, \langle \vec{x}_n \rangle)_P = (\vec{x}_{n\mathbb{R}}, \vec{x}_{n\mathbb{I}})_C, \end{aligned} \quad (2)$$

where $(\vec{x}_{n\mathbb{R}}, \vec{x}_{n\mathbb{I}})_C$ is in the 2D Cartesian notation and $(|\vec{x}_n|, \langle \vec{x}_n \rangle)_P$ is in the 2D polar notation. Each point-particle in P_X has a location that is a *2D Position-Point State* (2D-PPS) from [60, 61]. For P_X in eq. (1), we define

$$M_X = \{m_1, m_2, \dots, m_n\} \quad (3)$$

as the corresponding ordered set of non-zero *2D Position-Point-Masses* (2D-PPM) of cardinality $n = |M_X|$. Moreover, each point-particle in P_X also has a velocity that is a *2D Velocity Field Order Parameter State* (2D-VOPS) defined using the 2D-OPS notation of [60]. Hence, we define

$$V_X \equiv \{\vec{v}_1, \vec{v}_2, \dots, \vec{v}_n\} \equiv \{\vec{\psi}_v(\vec{x}_1), \vec{\psi}_v(\vec{x}_2), \dots, \vec{\psi}_v(\vec{x}_n)\} \quad (4)$$

as the ordered 2D-VOPS set of cardinality $n = |V_X|$ with the corresponding definitions

$$\begin{aligned} 1 : \vec{v}_1 &\equiv (\vec{v}_1) \equiv \vec{\psi}_v(\vec{x}_1) \equiv (|\vec{v}_1|, \langle \vec{v}_1 \rangle)_P \equiv (\vec{v}_{1\mathbb{R}}, \vec{v}_{1\mathbb{I}})_C \\ 2 : \vec{v}_2 &\equiv (\vec{v}_2) \equiv \vec{\psi}_v(\vec{x}_2) \equiv (|\vec{v}_2|, \langle \vec{v}_2 \rangle)_P \equiv (\vec{v}_{2\mathbb{R}}, \vec{v}_{2\mathbb{I}})_C \\ &\dots \\ n : \vec{v}_n &\equiv (\vec{v}_n) \equiv \vec{\psi}_v(\vec{x}_n) \equiv (|\vec{v}_n|, \langle \vec{v}_n \rangle)_P \equiv (\vec{v}_{n\mathbb{R}}, \vec{v}_{n\mathbb{I}})_C, \end{aligned} \quad (5)$$

where $(\vec{v}_{n_{\mathbb{R}}}, \vec{v}_{n_{\mathbb{I}}})_C$ is in the 2D Cartesian notation and $(|\vec{v}_n|, \langle \vec{v}_n \rangle)_P$ is in the 2D polar notation.

Next, we apply Newton's law of universal gravitation to M_X for P_X across X , where the force between between any two 2D-PPM is directly proportional to their product and inversely proportional to the square of the distance between them [1, 2]. To encode the gravitational force between two such bodies in the 3D IHR topology, say $m_i, m_j \in M_X$ for $i \neq j$ and $1 \leq i, j \leq n$, we adopt and adjust the 2D-OPS notation of eq. (23) in [60] and add a second 2D-PPS argument to define the *2D Newtonian Force Field Order Parameter State* (2D-FOPS)

$$\begin{aligned} \vec{F}_{ij} &\equiv \vec{F}_{ij_{\mathbb{R}}} + \vec{F}_{ij_{\mathbb{I}}} \equiv \left(\vec{F}_{ij} \right) \equiv \left(\vec{F}_{ij_{\mathbb{R}}}, \vec{F}_{ij_{\mathbb{I}}} \right)_C \equiv \left(|\vec{F}_{ij}|, \langle \vec{F}_{ij} \rangle \right)_P \\ &\equiv \vec{\psi}_F(\vec{x}_i, \vec{x}_j) \equiv \vec{\psi}_F(\vec{x}_i, \vec{x}_j)_{\mathbb{R}} + \vec{\psi}_F(\vec{x}_i, \vec{x}_j)_{\mathbb{I}} \equiv \left(\vec{\psi}_F(\vec{x}_i, \vec{x}_j) \right) \\ &\equiv \left(\vec{\psi}_F(\vec{x}_i, \vec{x}_j)_{\mathbb{R}}, \vec{\psi}_F(\vec{x}_i, \vec{x}_j)_{\mathbb{I}} \right)_C \equiv \left(|\vec{\psi}_F(\vec{x}_i, \vec{x}_j)|, \langle \vec{\psi}_F(\vec{x}_i, \vec{x}_j) \rangle \right)_P \end{aligned} \quad (6)$$

from the perspective of \vec{x}_i to \vec{x}_j , which applies to all such pairs in P_X . Hence, the 2D-OPS component constraints and notations of eqs. (18–25) in [60] apply to the 2D-FOPS definition of eq. (6). Therefore, $\forall \vec{x}_i, \vec{x}_j \in P_X$ the gravitational 2D-FOPS-amplitude between $m_i, m_j \in M_X$ is

$$\begin{aligned} |\vec{F}_{ij}| &\equiv \sqrt{\vec{F}_{ij_{\mathbb{R}}}^2 + \vec{F}_{ij_{\mathbb{I}}}^2} \equiv G \frac{m_i m_j}{d_{ij}^2} \\ &\equiv |\vec{\psi}_F(\vec{x}_i, \vec{x}_j)| \equiv \sqrt{\vec{\psi}_F^2(\vec{x}_i, \vec{x}_j)_{\mathbb{R}} + \vec{\psi}_F^2(\vec{x}_i, \vec{x}_j)_{\mathbb{I}}}, \end{aligned} \quad (7)$$

where G is the gravitational constant and d_{ij} is defined as the Euclidean distance

$$d_{ij} = d(\vec{x}_i, \vec{x}_j) = \sqrt{(\vec{x}_{j_{\mathbb{R}}} - \vec{x}_{i_{\mathbb{R}}})^2 + (\vec{x}_{j_{\mathbb{I}}} - \vec{x}_{i_{\mathbb{I}}})^2} \quad (8)$$

between \vec{x}_i and \vec{x}_j using the 2D-PPS Cartesian-coordinate properties for the geometrical line segment $\overline{\vec{x}_i \vec{x}_j}$.

Now, we can simplify the notation of eqs. (6–8) even further if we let $\vec{x}_i = O$ be the origin-point of eq. (10) in [60] with the 2D-PPM re-labeling

$m_O = m_i$. Thus, $\forall \vec{x}_j \in P_X$, eq. (6) is re-written as

$$\vec{F}_j \equiv \vec{\psi}_F(O, \vec{x}_j) \equiv \vec{F}_{j_R} + \vec{F}_{j_I} \equiv \left(\vec{F}_j \right) \equiv \left(\vec{F}_{j_R}, \vec{F}_{j_I} \right)_C \equiv \left(|\vec{F}_j|, \langle \vec{F}_j \rangle \right)_P, \quad (9)$$

with respect to O , which clearly satisfies the 2D-OPS component constraints and notations of eqs. (18–25) in [60]. Therefore, eq. (7) is re-written as

$$|\vec{F}_j| \equiv |\vec{\psi}_F(O, \vec{x}_j)| \equiv \sqrt{\vec{F}_{j_R}^2 + \vec{F}_{j_I}^2} \equiv G \frac{m_O m_j}{d_j^2}, \quad (10)$$

where d_j is defined as the Euclidean distance by re-writing eq. (8) as

$$d_j = d(O, \vec{x}_j) = \sqrt{(\vec{x}_{j_R} - O_R)^2 + (\vec{x}_{j_I} - O_I)^2} = |\vec{x}_j| \quad (11)$$

between O and \vec{x}_j , which is the 2D-PPS-amplitude that corresponds to the geometrical line segment $\overline{O\vec{x}_j}$.

At this point, we have both the \vec{F}_j of eq. (9) and the $m_j \in M_X$ of eq. (3), so Newton's second law [1, 2] immediately comes to mind. Thus, using the same notation of eq. (9), we define the *2D Newtonian Acceleration Field Order Parameter State* (2D-AOPS)

$$\vec{a}_j \equiv \vec{\psi}_a(O, \vec{x}_j) \equiv (\vec{a}_j) \equiv (\vec{a}_{j_R}, \vec{a}_{j_I})_C \equiv (|\vec{a}_j|, \langle \vec{a}_j \rangle)_P, \quad (12)$$

with respect to O , where the 2D-AOPS-amplitude is defined as

$$|\vec{a}_j| \equiv |\vec{\psi}_a(O, \vec{x}_j)| \equiv \sqrt{\vec{a}_{j_R}^2 + \vec{a}_{j_I}^2} \equiv \frac{|\vec{F}_j|}{m_j}. \quad (13)$$

Hence, for $m_0, m_j \in M_X$, the 2D-FOPS-phase, 2D-AOPS-phase, and 2D-PPS-phase bestow the equivalence

$$\langle \vec{F}_j \rangle \equiv \langle \vec{a}_j \rangle \equiv \langle \vec{x}_j \rangle. \quad (14)$$

The next step is to define, relative to m_O with v_O , the *2D Relative Velocity Field Order Parameter State* (2D-RVOPS) for some m_j with v_j as

$$\vec{v}_j \equiv \vec{\psi}_v(O, \vec{x}_j) \equiv \left(\vec{v}_j \right) \equiv \left(\vec{v}_{j_R}, \vec{v}_{j_I} \right)_C \equiv \left(|\vec{v}_j|, \langle \vec{v}_j \rangle \right)_P, \quad (15)$$

such that

$$\begin{aligned}\vec{\vartheta}_{j_{\mathbb{R}}} &\equiv \vec{v}_{j_{\mathbb{R}}} - \vec{v}_{O_{\mathbb{R}}} \\ \vec{\vartheta}_{j_{\mathbb{I}}} &\equiv \vec{v}_{j_{\mathbb{I}}} - \vec{v}_{O_{\mathbb{I}}},\end{aligned}\tag{16}$$

where from eq. (22) in [60] we establish

$$\begin{aligned}|\vec{\vartheta}_j| &\equiv \sqrt{\vec{\vartheta}_{j_{\mathbb{R}}}^2 + \vec{\vartheta}_{j_{\mathbb{I}}}^2} \\ \vec{\vartheta}_{j_{\mathbb{R}}} &\equiv |\vec{\vartheta}_j| \cos\langle\vec{\vartheta}_j\rangle \\ \vec{\vartheta}_{j_{\mathbb{I}}} &\equiv |\vec{\vartheta}_j| \sin\langle\vec{\vartheta}_j\rangle,\end{aligned}\tag{17}$$

which is clearly similar to the constraints of eqs. (9) and (12) that follow [60]. Eqs. (15–17) are preliminary relative velocity definitions that are sufficient to introduce the NGNBSSA for the limited context of this introductory paper; however, in future work it should be interesting and beneficial to incorporate additional aspects of Einstein’s special relativity into this developing framework.

We note that the 1-sphere IHR $T^1 \subset X$ in eq. (13) of [60] with amplitude-radius ϵ does apply to this scenario, but we must wait to establish T^1 in Section 3.1 because the value of ϵ depends on the NGNBSSA’s intermediate results. A 2D-PPS that exists in T^1 is defined as an *IHRE-2D-PPS*; the 2D-PPM, 2D-FOPS, 2D-AOPS, 2D-VOPS, and 2D-RVOPS for an *IHRE-2D-PPS* are defined as the *IHRE-2D-PPM*, *IHRE-2D-FOPS*, *IHRE-2D-AOPS*, *IHRE-2D-VOPS*, and *IHRE-2D-RVOPS*, respectively. Thus, at this point, we can encode the relevant n -body chaotic dynamical system states in the 3D IHR topology of [60, 61] for the upcoming NGNBSSA in Section 3.1.

2.2 3D structures in the 4D IHR topology

Here, we project the complex structures of Section 2.1 to a higher dimensional structure with one additional degree of freedom.

First, we project the 2D locations of eqs. (1–2) in accordance to [60]. Thus, to encode 3D locations, we identify the 3D real manifold Y as the 3D

Position-Point State Space (3D-PPSS), such that $X \subset Y$ [60]. Thus, we define

$$P_Y \subset Y = \{\vec{y}_1, \vec{y}_2, \dots, \vec{y}_n\} \quad (18)$$

as the ordered set of spherically-symmetric point-particles of cardinality $n = |P_Y|$ with the corresponding generalized *3D Riemannian-coordinates* [60]

$$\begin{aligned} 1 : \vec{y}_1 &= (\vec{y}_1) = (|\vec{y}_1|, \langle \vec{y}_1 \rangle, [\vec{y}_1])_S = (\vec{y}_{1_R}, \vec{y}_{1_I}, \vec{y}_{1_Z})_C \\ 2 : \vec{y}_2 &= (\vec{y}_2) = (|\vec{y}_2|, \langle \vec{y}_2 \rangle, [\vec{y}_2])_S = (\vec{y}_{2_R}, \vec{y}_{2_I}, \vec{y}_{2_Z})_C \\ &\dots \\ n : \vec{y}_n &= (\vec{y}_n) = (|\vec{y}_n|, \langle \vec{y}_n \rangle, [\vec{y}_n])_S = (\vec{y}_{n_R}, \vec{y}_{n_I}, \vec{y}_{n_Z})_C, \end{aligned} \quad (19)$$

where $(|\vec{y}_n|, \langle \vec{y}_n \rangle, [\vec{y}_n])_S$ is in the 3D spherical notation and $(\vec{y}_{n_R}, \vec{y}_{n_I}, \vec{y}_{n_Z})_C$ is in the 3D Cartesian notation. Each point-particle in P_Y has a location that is a *3D Position-Point State* (3D-PPS) from [60]. For P_Y in eq. (18), we define

$$M_Y = \{m_1, m_2, \dots, m_n\} \quad (20)$$

as the corresponding ordered set of non-zero *3D Position-Point-Masses* (3D-PPM) of cardinality $n = |M_Y|$. Moreover, each point-particle in P_Y also has a velocity that is a *3D Velocity Field Order Parameter State* (3D-VOPS) defined using the 3D-OPS notation of [60]. Hence, we define

$$V_Y = \{\vec{v}_1, \vec{v}_2, \dots, \vec{v}_n\} = \{\vec{\psi}_v(\vec{y}_1), \vec{\psi}_v(\vec{y}_2), \dots, \vec{\psi}_v(\vec{y}_n)\} \quad (21)$$

as the ordered 3D-VOPSs set of cardinality $n = |V_Y|$ with the corresponding definitions

$$\begin{aligned} 1 : \vec{v}_1 &\equiv (\vec{v}_1) \equiv \vec{\psi}_v(\vec{y}_1) \equiv (|\vec{v}_1|, \langle \vec{v}_1 \rangle, [\vec{v}_1])_S \equiv (\vec{v}_{1_R}, \vec{v}_{1_I}, \vec{v}_{1_Z})_C \\ 2 : \vec{v}_2 &\equiv (\vec{v}_2) \equiv \vec{\psi}_v(\vec{y}_2) \equiv (|\vec{v}_2|, \langle \vec{v}_2 \rangle, [\vec{v}_2])_S \equiv (\vec{v}_{2_R}, \vec{v}_{2_I}, \vec{v}_{2_Z})_C \\ &\dots \\ n : \vec{v}_n &\equiv (\vec{v}_n) \equiv \vec{\psi}_v(\vec{y}_n) \equiv (|\vec{v}_n|, \langle \vec{v}_n \rangle, [\vec{v}_n])_S \equiv (\vec{v}_{n_R}, \vec{v}_{n_I}, \vec{v}_{n_Z})_C. \end{aligned} \quad (22)$$

Next, we apply Newton's law of universal gravitation [1, 2] to M_Y for P_Y across Y . To encode the gravitational force between two such 3D-PPMs in the 4D IHR topology, say $m_i, m_j \in M_Y$ for $i \neq j$ and $1 \leq i, j \leq n$, we

adopt and adjust the 3D-OPS notation of eq. (50) in [60] and add a second 3D-PPS argument to define the *3D Newtonian Force Field Order Parameter State* (3D-FOPS)

$$\begin{aligned}
\vec{F}_{ij} &\equiv \vec{F}_{ij_{\mathbb{R}}} + \vec{F}_{ij_{\mathbb{I}}} + \vec{F}_{ij_{\mathbb{Z}}} \equiv \left(\vec{F}_{ij} \right) \equiv \left(\vec{F}_{ij_{\mathbb{R}}}, \vec{F}_{ij_{\mathbb{I}}}, \vec{F}_{ij_{\mathbb{Z}}} \right)_C \equiv \left(|\vec{F}_{ij}|, \langle \vec{F}_{ij} \rangle, [\vec{F}_{ij}] \right)_S \\
&\equiv \vec{\psi}_F(\vec{y}_i, \vec{y}_j) \equiv \vec{\psi}_F(\vec{y}_i, \vec{y}_j)_{\mathbb{R}} + \vec{\psi}_F(\vec{y}_i, \vec{y}_j)_{\mathbb{I}} + \vec{\psi}_F(\vec{y}_i, \vec{y}_j)_{\mathbb{Z}} \equiv \left(\vec{\psi}_F(\vec{y}_i, \vec{y}_j) \right)_S \\
&\equiv \left(\vec{\psi}_F(\vec{y}_i, \vec{y}_j)_{\mathbb{R}}, \vec{\psi}_F(\vec{y}_i, \vec{y}_j)_{\mathbb{I}}, \vec{\psi}_F(\vec{y}_i, \vec{y}_j)_{\mathbb{Z}} \right)_C \\
&\equiv \left(|\vec{\psi}_F(\vec{y}_i, \vec{y}_j)|, \langle \vec{\psi}_F(\vec{y}_i, \vec{y}_j) \rangle, [\vec{\psi}_F(\vec{y}_i, \vec{y}_j)] \right)_S
\end{aligned} \tag{23}$$

from the perspective of \vec{y}_i to \vec{y}_j , which applies to all such pairs in P_Y . Hence, the 3D-OPS component constraints and notations of eqs. (45–52) in [60] apply to the 3D-FOPS definition of eq. (23). Therefore, $\forall \vec{y}_i, \vec{y}_j \in P_Y$ the gravitational 3D-FOPS-amplitude between $m_i, m_j \in M_Y$ is

$$\begin{aligned}
|\vec{F}_{ij}| &\equiv \sqrt{\vec{F}_{ij_{\mathbb{R}}}^2 + \vec{F}_{ij_{\mathbb{I}}}^2 + \vec{F}_{ij_{\mathbb{Z}}}^2} \equiv G \frac{m_i m_j}{d_{ij}^2} \\
&\equiv |\vec{\psi}_F(\vec{y}_i, \vec{y}_j)| \equiv \sqrt{\vec{\psi}_F^2(\vec{y}_i, \vec{y}_j)_{\mathbb{R}} + \vec{\psi}_F^2(\vec{y}_i, \vec{y}_j)_{\mathbb{I}} + \vec{\psi}_F^2(\vec{y}_i, \vec{y}_j)_{\mathbb{Z}}},
\end{aligned} \tag{24}$$

where d_{ij} is defined as the Euclidean distance

$$d_{ij} = d(\vec{y}_i, \vec{y}_j) = \sqrt{(\vec{y}_{j_{\mathbb{R}}} - \vec{y}_{i_{\mathbb{R}}})^2 + (\vec{y}_{j_{\mathbb{I}}} - \vec{y}_{i_{\mathbb{I}}})^2 + (\vec{y}_{j_{\mathbb{Z}}} - \vec{y}_{i_{\mathbb{Z}}})^2} \tag{25}$$

between \vec{y}_i and \vec{y}_j using the 3D-PPS Cartesian-coordinate properties for the geometrical line segment $\overline{\vec{y}_i \vec{y}_j}$.

Now, we can simplify the notation of eqs. (23–25) even further if we let $\vec{y}_i = O$ be the 3D version of the origin-point in [60] with the 3D-PPM re-labeling $m_O = m_i$. Thus, $\forall \vec{y}_j \in P_Y$, eq. (23) is re-written as

$$\vec{F}_j \equiv \vec{\psi}_F(O, \vec{y}_j) \equiv \vec{F}_{j_{\mathbb{R}}} + \vec{F}_{j_{\mathbb{I}}} + \vec{F}_{j_{\mathbb{Z}}} \equiv \left(\vec{F}_j \right) \equiv \left(\vec{F}_{j_{\mathbb{R}}}, \vec{F}_{j_{\mathbb{I}}}, \vec{F}_{j_{\mathbb{Z}}} \right)_C \equiv \left(|\vec{F}_j|, \langle \vec{F}_j \rangle, [\vec{F}_j] \right)_S, \tag{26}$$

with respect to O , which clearly satisfies the 3D-OPS component constraints and notations of eqs. (45–52) in [60]. Therefore, eq. (24) is re-written as

$$|\vec{F}_j| \equiv |\vec{\psi}_F(O, \vec{y}_j)| \equiv \sqrt{\vec{F}_{j\mathbb{R}}^2 + \vec{F}_{j\mathbb{I}}^2 + \vec{F}_{j\mathbb{Z}}^2} \equiv G \frac{m_O m_j}{d_j^2}, \quad (27)$$

where d_j is defined as the Euclidean distance by re-writing eq. (25) as

$$d_j = d(O, \vec{y}_j) = \sqrt{(\vec{y}_{j\mathbb{R}} - O_{\mathbb{R}})^2 + (\vec{y}_{j\mathbb{I}} - O_{\mathbb{I}})^2 + (\vec{y}_{j\mathbb{Z}} - O_{\mathbb{Z}})^2} = |\vec{y}_j| \quad (28)$$

between O and \vec{y}_j , which is the 3D-PPS-amplitude that corresponds to the geometrical line segment $\overline{O\vec{y}_j}$.

At this point, we have both the \vec{F}_j of eq. (26) and the $m_j \in M_Y$ of eq. (20), so again we recall Newton's second law [1, 2]. Thus, using the same notation of eq. (26), we define the *3D Newtonian Acceleration Field Order Parameter State* (3D-AOPS)

$$\vec{a}_j \equiv \vec{\psi}_a(O, \vec{x}_j) \equiv (\vec{a}_j) \equiv (\vec{a}_{j\mathbb{R}}, \vec{a}_{j\mathbb{I}}, \vec{a}_{j\mathbb{Z}})_C \equiv (|\vec{a}_j|, \langle \vec{a}_j \rangle, [\vec{a}_j])_S, \quad (29)$$

with respect to O , where the 3D-AOPS-amplitude is defined as

$$|\vec{a}_j| \equiv |\vec{\psi}_a(O, \vec{x}_j)| \equiv \sqrt{\vec{a}_{j\mathbb{R}}^2 + \vec{a}_{j\mathbb{I}}^2 + \vec{a}_{j\mathbb{Z}}^2} \equiv \frac{|\vec{F}_j|}{m_j}. \quad (30)$$

Hence, for $m_0, m_j \in M_Y$, the 3D-FOPS-phase, 3D-AOPS-phase, and 3D-PPS-phase bestow the equivalence

$$\langle \vec{F}_j \rangle \equiv \langle \vec{a}_j \rangle \equiv \langle \vec{y}_j \rangle, \quad (31)$$

while the 3D-FOPS-inclination, 3D-AOPS-inclination, and 3D-PPS-inclination similarly yield

$$[\vec{F}_j] \equiv [\vec{a}_j] \equiv [\vec{y}_j]. \quad (32)$$

The next step is to define, relative to m_O with v_O , the *3D Relative Velocity Field Order Parameter State* (3D-RVOPS) for some m_j with v_j as

$$\vec{v}_j \equiv \vec{\psi}_v(O, \vec{y}_j) \equiv (\vec{v}_j) \equiv (\vec{v}_{j\mathbb{R}}, \vec{v}_{j\mathbb{I}}, \vec{v}_{j\mathbb{Z}})_C \equiv (|\vec{v}_j|, \langle \vec{v}_j \rangle, [\vec{v}_j])_S, \quad (33)$$

such that

$$\begin{aligned}
\vec{\vartheta}_{j_{\mathbb{R}}} &\equiv \vec{v}_{j_{\mathbb{R}}} - \vec{v}_{O_{\mathbb{R}}} \\
\vec{\vartheta}_{j_{\mathbb{I}}} &\equiv \vec{v}_{j_{\mathbb{I}}} - \vec{v}_{O_{\mathbb{I}}} \\
\vec{\vartheta}_{j_{\mathbb{Z}}} &\equiv \vec{v}_{j_{\mathbb{Z}}} - \vec{v}_{O_{\mathbb{Z}}},
\end{aligned} \tag{34}$$

where from eq. (49) in [60] we establish

$$\begin{aligned}
|\vec{\vartheta}_j| &\equiv \sqrt{\vec{\vartheta}_{j_{\mathbb{R}}}^2 + \vec{\vartheta}_{j_{\mathbb{I}}}^2 + \vec{\vartheta}_{j_{\mathbb{Z}}}^2} \\
\langle \vec{\vartheta}_j \rangle &\equiv \arctan\left(\frac{\vec{\vartheta}_{j_{\mathbb{I}}}}{\vec{\vartheta}_{j_{\mathbb{R}}}}\right) \\
[\vec{\vartheta}_j] &\equiv \arccos\left(\frac{\vec{\vartheta}_{j_{\mathbb{Z}}}}{|\vec{\vartheta}_j|}\right),
\end{aligned} \tag{35}$$

which is clearly similar to the constraints of eqs. (26) and (29) that follow [60]. Eq. (35) illustrates the conventional conversion relation between 3D spherical and 3D Cartesian components, and would be most useful with a well-behaved 3D/triplex algebra [60] that is still under development.

We note that the 2-sphere IHR $T^2 \subset Y$ in eq. (40) of [60] with amplitude-radius ϵ does apply to this scenario, but we must wait to establish T^2 in Section 3.2 because the value of ϵ depends on the NGNBSSA's intermediate results. A 3D-PPS that exists in T^2 is defined as a *IHRE-3D-PPS*; the 3D-PPM, 3D-FOPS, 3D-AOPS, 3D-VOPS, and 3D-RVOPS for an *IHRE-3D-PPS* are defined as the *IHRE-3D-PPM*, *IHRE-3D-FOPS*, *IHRE-3D-AOPS*, *IHRE-3D-VOPS*, and *IHRE-3D-RVOPS*, respectively. Thus, at this point, we can encode the relevant n -body chaotic dynamical system states in the 4D IHR topology of [60] for the upcoming NGNBSSA in Section 3.2.

3 Algorithm

In this section, we explain *how* certain aspects of Newton's ($n > 2$)-PPM problem can be reduced to a ($n = 2$)-PPM problem for compliance with the holographic principle [63]; for this, the complete NGNBSSA is communicated via an example with step-by-step diagrams. The NGNBSSA's ulti-

mate objective is to partition the $(n > 2)$ -PPMs into 2-PPMs: the *Origin Position-Point-Mass* (O-PPM) and the *IHRE Position-Point-Mass* (IHRE-PPM) Singleton. To summarize this process, we arbitrarily select one PPM to be the origin centered on O , namely the O-PPM, and subsequently engage a series of *IHRE Normalization Adjustment* (IHRE-NA) instructions to consolidate the residual $(n - 1)$ -PPMs to a single, consolidated IHRE-PPM, where the location and feature vectors of the $(n - 1)$ -PPMs are summed to produce net vectors with effective quantities. The IHRE-PPM along T^1 (or T^2 in the 4D IHR case) represents the spherically-symmetric effective mass centered on O with amplitude-radius ϵ from [60, 61] for which the gravitational force and relative effects are preserved under the IHRE-NAs. From there, we demonstrate that it is possible calculate the *net* IHRE quantities between the O-PPM and the IHRE-PPM so we may exercise the IHRE potential, kinetic, and Lagrangian definitions in the IHR topology [61].

In this systematic illustration, we choose to solve the $(n = 3)$ -PPM base case in the 3D IHR topology due to its visualization simplicity—it is easier to draw Figures 1–6 on X and reduce 3-PPMs to 2-PPMs. But as we shall see, the guidelines of the NGNBSSA are kept generalized and can be directly applied to $(n > 3)$ -PPMs. Moreover, the NGNBSSA is *almost identical* for both 3D and 4D IHR topology scenarios. Thus, in Section 3.1, we introduce and define the NGNBSSA with step-by-step depictions for the 3D IHR topology with $T^1 \subset X$ [60, 61]. Then in Section 3.2, we explain precisely how to apply it to 4D IHR topology with $T^2 \subset Y$ [60] by simply “swapping out” the data structures and making a couple of slight algorithmic adjustments.

3.1 2D algorithm for the 3D IHR topology

The $(n = 3)$ -PPM illustration for the NGNBSSA in the 3D IHR topology is defined by the following sequence:

- ***Routine 1:*** Initializing the n -Body Particles
 1. Randomly generate or experimentally identify $n = 3$ distinct PPSs on X to create the ordered PPS set P_X in the form of eq. (1) with the 2D Riemannian-coordinates of eq. (2); *we let these*

2D-PPSs be

$$P_X \subset X = \{\vec{x}_A, \vec{x}_B, \vec{x}_C\}$$

(for this example, we assert that \vec{x}_B and \vec{x}_C are different distances from \vec{x}_A for illustration purposes, but certainly this is not a necessary requirement).

2. Randomly assign or experimentally measure the three PPMs to create the ordered PPM set M_X in the form of eq. (3) that correspond to the established PPSs of P_X ; let

$$M_X = \{m_A, m_B, m_C\}$$

be the ordered 2D-PPM set of three 2D-PPM elements that respectively correspond to P_X , such that $m_A, m_B, m_C > 0$.

3. Randomly assign or experimentally measure the three VOPSs to create the ordered VOPS set V_X of eq. (4) in the form of eq. (5) that correspond to the established PPSs of P_X ; let

$$V_X = \{\vec{v}_A, \vec{v}_B, \vec{v}_C\}$$

be the ordered 2D-VOPS set of three 2D-VOPS elements that respectively correspond to P_X .

4. See Figure 1.

- **Routine 2:** Initializing the IHR Topology

1. Arbitrarily select a PPS from P_X ; let us choose $\vec{x}_A \in P_X$.
2. Determine the closest PPS to the selected \vec{x}_A using the Euclidean distance; using the 2D Euclidean distance of eq. (8) we determine that $\vec{x}_B \in P_X$ is the closest to the selected \vec{x}_A , where the distance between them is d_{AB} .
3. Draw the 1-sphere IHR $T^1 \subset X$ to represent the “time zone” from eq. (13) in [60], where the selected \vec{x}_A is T^1 's center, such that \vec{x}_B lies precisely on T^1 ; we construct the 1-sphere IHR $T^1 \subset X$ with center \vec{x}_A , where T^1 's amplitude-radius ϵ from eq. (15) in [60] is equal to the Euclidean distance d_{AB} between \vec{x}_A and \vec{x}_B , so $d_{AB} = \epsilon$ for the geometrical line segment $\overline{\vec{x}_A \vec{x}_B}$, such that $\vec{x}_B \in T^1$.

4. Label the spatial sub-surfaces that are simultaneously dual to T^1 ; T^1 topologically delineates the “micro space zone” $X_- \subset X$ and “macro space zone” $X_+ \subset X$ for the “space-time duality” of the IHR topology in [60, 61].

5. See Figure 2.

- **Routine 3:** Initializing the O-PPM and Reference Frame, and Assigning the OPSs

1. Designate the selected \vec{x}_A as the origin-point O of X to establish the reference frame; we re-name \vec{x}_A as O to thereby assign $O = \vec{x}_A$ as the origin and point-of-reference, and additionally re-name the PPM m_A as the O-PPM of X to thereby assign $m_O = m_A$.
2. Use eqs. (9–10) to assign FOPSs to the PPM that is the closest to m_O (namely m_B at \vec{x}_B) and all remaining PPMs in M_X (which is just m_C at \vec{x}_C because $n = 3$); for O and \vec{x}_B , the 2D-FOPS between the corresponding m_O and m_B is

$$\vec{F}_B = \vec{F}_{B_{\mathbb{R}}} + \vec{F}_{B_{\mathbb{I}}} = (\vec{F}_B) = (|\vec{F}_B|, \langle \vec{F}_B \rangle)_P = (\vec{F}_{B_{\mathbb{R}}}, \vec{F}_{B_{\mathbb{I}}})_C,$$

such that

$$|\vec{F}_B| = G \frac{m_O m_B}{|\vec{x}_B|^2} = G \frac{m_O m_B}{|d_B|^2} = G \frac{m_O m_B}{\epsilon^2}$$

$$\langle \vec{F}_B \rangle = \langle \vec{x}_B \rangle,$$

and for O and \vec{x}_C , the 2D-FOPS between the corresponding m_O and m_C is

$$\vec{F}_C = \vec{F}_{C_{\mathbb{R}}} + \vec{F}_{C_{\mathbb{I}}} = (\vec{F}_C) = (|\vec{F}_C|, \langle \vec{F}_C \rangle)_P = (\vec{F}_{C_{\mathbb{R}}}, \vec{F}_{C_{\mathbb{I}}})_C,$$

such that

$$|\vec{F}_C| = G \frac{m_O m_C}{|\vec{x}_C|^2} = G \frac{m_O m_B}{|d_C|^2}$$

$$\langle \vec{F}_C \rangle = \langle \vec{x}_C \rangle.$$

3. Use eqs. (12–13) to assign AOPSs to $m_B, m_C \in M_X$, with respect to m_O ; for O and \vec{x}_B , the 2D-AOPS between the corresponding m_O and m_B is

$$\vec{a}_B = \vec{a}_{B_{\mathbb{R}}} + \vec{a}_{B_{\mathbb{I}}} = (\vec{a}_B) = (|\vec{a}_B|, \langle \vec{a}_B \rangle)_P = (\vec{a}_{B_{\mathbb{R}}}, \vec{a}_{B_{\mathbb{I}}})_C,$$

such that

$$\begin{aligned} |\vec{a}_B| &= \frac{|\vec{F}_B|}{m_B} \\ \langle \vec{a}_B \rangle &= \langle \vec{F}_B \rangle = \langle \vec{x}_B \rangle, \end{aligned}$$

and for O and \vec{x}_C , the 2D-AOPS between the corresponding m_O and m_C is

$$\vec{a}_C = \vec{a}_{C_{\mathbb{R}}} + \vec{a}_{C_{\mathbb{I}}} = (\vec{a}_C) = (|\vec{a}_C|, \langle \vec{a}_C \rangle)_P = (\vec{a}_{C_{\mathbb{R}}}, \vec{a}_{C_{\mathbb{I}}})_C,$$

such that

$$\begin{aligned} |\vec{a}_C| &= \frac{|\vec{F}_C|}{m_B} \\ \langle \vec{a}_C \rangle &= \langle \vec{F}_C \rangle = \langle \vec{x}_C \rangle. \end{aligned}$$

4. Relative to m_O with \vec{v}_O , use eqs. (15–17) to assign RVOPSs to $m_B, m_C \in M_X$ with $\vec{v}_B, \vec{v}_C \in V_X$; for O and \vec{x}_B , the 2D-RVOPS for the corresponding \vec{v}_O and \vec{v}_B is

$$\vec{v}_B = \vec{v}_{B_{\mathbb{R}}} + \vec{v}_{B_{\mathbb{I}}} = (\vec{v}_B) = (|\vec{v}_B|, \langle \vec{v}_B \rangle)_P = (\vec{v}_{B_{\mathbb{R}}}, \vec{v}_{B_{\mathbb{I}}})_C,$$

such that

$$\begin{aligned} \vec{v}_{B_{\mathbb{R}}} &= \vec{v}_{B_{\mathbb{R}}} - \vec{v}_{O_{\mathbb{R}}} &= |\vec{v}_B| \cos \langle \vec{v}_B \rangle \\ \vec{v}_{B_{\mathbb{I}}} &= \vec{v}_{B_{\mathbb{I}}} - \vec{v}_{O_{\mathbb{I}}} &= |\vec{v}_B| \sin \langle \vec{v}_B \rangle \\ |\vec{v}_B| &= \sqrt{\vec{v}_{B_{\mathbb{R}}}^2 + \vec{v}_{B_{\mathbb{I}}}^2}, \end{aligned}$$

and for O and \vec{x}_C , the 2D-RVOPS for the corresponding \vec{v}_O and \vec{v}_C is

$$\vec{v}_C = \vec{v}_{C_{\mathbb{R}}} + \vec{v}_{C_{\mathbb{I}}} = (\vec{v}_C) = (|\vec{v}_C|, \langle \vec{v}_C \rangle)_P = (\vec{v}_{C_{\mathbb{R}}}, \vec{v}_{C_{\mathbb{I}}})_C,$$

such that

$$\begin{aligned}\vec{\vartheta}_{C_{\mathbb{R}}} &= \vec{v}_{C_{\mathbb{R}}} - \vec{v}_{O_{\mathbb{R}}} &= |\vec{\vartheta}_C| \cos\langle\vec{\vartheta}_C\rangle \\ \vec{\vartheta}_{C_{\mathbb{I}}} &= \vec{v}_{C_{\mathbb{I}}} - \vec{v}_{O_{\mathbb{I}}} &= |\vec{\vartheta}_C| \sin\langle\vec{\vartheta}_C\rangle \\ |\vec{\vartheta}_C| &= \sqrt{\vec{\vartheta}_{C_{\mathbb{R}}}^2 + \vec{\vartheta}_{C_{\mathbb{I}}}^2}.\end{aligned}$$

5. See Figure 3.

• **Routine 4:** Constructing the IHRE-PPM Set

1. Use X 's built-in IHR duality of eq. (17) in [60] to map all the PPMs that are currently in X_+ to T^1 to acquire the IHRE-PPSs that share the uniform amplitude-radii ϵ , namely the *IHRE-PPS Set* of the *IHRE-PPM Set*, for spherically-symmetric normalization, where these mappings are IHRE-NAs that satisfy the two *IHRE-NA Constraints*:

- IHRE-NA Phase Constraint: when the external PPMs in X_+ are mapped to their corresponding IHRE-PPMs in T^1 , the phase of the PPS, IHRE-PPS, FOPS, IHRE-FOPS, AOPS, and IHRE-AOPS must be equivalent for each PPM transformation (to preserve the directional effect), and
- IHRE-NA Amplitude Constraint: when the external PPMs in X_+ are mapped to their corresponding IHRE-PPMs in T^1 , the amplitude of the FOPS and IHRE-FOPS must be equivalent (to preserve the gravitational force effect);

for the PPM m_C at the PPS $\vec{x}_C \in X_+$, we identify and create the corresponding IHRE-PPM m_{C^*} at the IHRE-PPS $\vec{x}_{C^*} \in T^1$, with the PPS IHRE-NA

$$\vec{x}_C \rightarrow \vec{x}_{C^*}, \quad (36)$$

and select/calculate the corresponding IHRE-PPM solution m_{C^*} , such that $m_{C^*} \neq m_C$, which satisfies the (2D) IHRE-NA Phase Constraint

$$\begin{aligned}\langle\vec{x}_{C^*}\rangle &= \langle\vec{x}_C\rangle = \langle\vec{F}_{C^*}\rangle = \langle\vec{F}_C\rangle = \langle\vec{a}_{C^*}\rangle = \langle\vec{a}_C\rangle \\ |\vec{x}_{C^*}| &\neq |\vec{x}_C| \Rightarrow \vec{x}_{C^*} \neq \vec{x}_C,\end{aligned} \quad (37)$$

and also satisfies the IHRE-NA Amplitude Constraint

$$\begin{aligned}
|\vec{F}_{C^*}| &= |\vec{F}_C| = G \frac{m_O m_{C^*}}{d_{C^*}^2} = G \frac{m_O m_C}{d_C^2} = m_C |\vec{a}_C| = m_{C^*} |\vec{a}_{C^*}| \\
m_{C^*} &\neq m_C, \quad d_{C^*} \neq d_C, \quad d_{C^*} = \epsilon, \quad d_C \neq \epsilon \\
(|\vec{F}_{C^*}| &= |\vec{F}_C|) \wedge (d_{C^*} \neq d_C) \Rightarrow (m_{C^*} \neq m_C),
\end{aligned} \tag{38}$$

m_B and m_{C^*} comprise the resulting IHRE-PPM Set for \vec{x}_B and \vec{x}_{C^*} , respectively, of the corresponding IHRE-PPS Set.

2. See Figure 4.

• **Routine 5:** Constructing the Initial IHRE-PPM Singleton

1. For the newly acquired Initial IHRE-PPM Set (all IHRE-PPMs currently in T^1), sum the corresponding IHRE-PPSs to calculate the *net PPS* of the Initial IHRE-PPM Singleton; for the IHRE-PPMs m_B and m_{C^*} in T^1 , we sum the corresponding IHRE-PPSs $\{\vec{x}_B, \vec{x}_{C^*}\} \in T^1$ to determine the *net PPS*

$$\vec{x}_D = \vec{x}_{net} = \vec{x}_B + \vec{x}_{C^*} \tag{39}$$

for the Initial IHRE-PPM Singleton m_D .

2. For the Initial IHRE-PPM Set, sum the corresponding IHRE-FOPSs to calculate the *net FOPS* of the Initial IHRE-PPM Singleton; for the IHRE-PPMs m_B and m_{C^*} in T^1 , we sum the corresponding FOPSs \vec{F}_B and \vec{F}_{C^*} to determine the *net FOPS*

$$\vec{F}_D = \vec{F}_{net} = \vec{F}_B + \vec{F}_{C^*}, \tag{40}$$

such that the *net FOPS amplitude* is

$$|\vec{F}_D| = |\vec{F}_{net}| = G \frac{m_O m_D}{|\vec{x}_D|^2} = G \frac{m_O m_D}{d_D^2} = G \frac{m_O m_{net}}{d_{net}^2} \tag{41}$$

and the corresponding *net FOPS phase* is

$$\langle \vec{F}_D \rangle = \langle \vec{F}_{net} \rangle = \langle \vec{x}_D \rangle = \langle \vec{x}_{net} \rangle \tag{42}$$

for the Initial IHRE-PPM Singleton $m_D = m_{net}$.

3. For the Initial IHRE-PPM Singleton m_D , use the results of eqs. (39–42) to calculate the *net AOPS*; for the *Initial IHRE-PPM Singleton* m_D , the *net AOPS* $\vec{a}_D = \vec{a}_{net}$ has the *net AOPS amplitude*

$$|\vec{a}_D| = |\vec{a}_{net}| = \frac{|\vec{F}_D|}{m_D} = \frac{|\vec{F}_{net}|}{m_{net}} \quad (43)$$

and the *net AOPS phase*

$$\langle \vec{a}_D \rangle = \langle \vec{a}_{net} \rangle = \langle \vec{F}_D \rangle = \langle \vec{F}_{net} \rangle = \langle \vec{x}_D \rangle = \langle \vec{x}_{net} \rangle, \quad (44)$$

so now there are just two PPMs to deal with, namely m_O and m_D !

4. Determine if the Initial IHRE-PPM Singleton m_D qualifies as a Final IHRE-PPM Singleton, which means that \vec{x}_D must be precisely on T^1 (this is an edge case); we observe that $\vec{x}_D \notin T^1$ and $\vec{x}_D \neq O$, but rather $\vec{x}_D \in X_+$, so m_D is not a Final IHRE-PPM Singleton and therefore we must proceed to Routine 6 to obtain some final m_{D^*} by re-applying the IHRE-NAs one last time.
5. See Figure 5.

• **Routine 6:** Constructing the Final IHRE-PPM Singleton

1. Similarly to Routine 4, we employ X 's built-in IHR duality to IHRE-NA map the Initial IHRE-PPM Singleton m_D to its corresponding Final IHRE-PPM Singleton m_{D^*} to establish the Final IHRE-PPS requirement $\vec{x}_{D^*} \in T^1$ in accordance to the IHRE-NA Constraints; for the *Initial IHRE-PPS Singleton* $\vec{x}_D \in X_+$ we identify the corresponding *Initial IHRE-PPS Singleton* $\vec{x}_{D^*} \in T^1$ via the mapping adjustment

$$\vec{x}_D \rightarrow \vec{x}_{D^*} \quad (45)$$

and thereby select/calculate the corresponding *Final IHRE-PPM Singleton* m_{D^*} , such that $m_{D^*} \neq m_D$, which satisfies the IHRE-

NA Phase Constraint

$$\begin{aligned} \langle \vec{x}_{D^*} \rangle &= \langle \vec{x}_D \rangle = \langle \vec{F}_{D^*} \rangle = \langle \vec{F}_D \rangle = \langle \vec{a}_{D^*} \rangle = \langle \vec{a}_D \rangle \\ |\vec{x}_{D^*}| &\neq |\vec{x}_D| \Rightarrow \vec{x}_{D^*} \neq \vec{x}_D, \end{aligned} \quad (46)$$

and also satisfies the IHRE-NA Amplitude Constraint

$$\begin{aligned} |\vec{F}_{D^*}| &= |\vec{F}_D| = G \frac{m_O m_{D^*}}{d_{D^*}^2} = G \frac{m_O m_D}{d_D^2} = m_D |\vec{a}_D| = m_{D^*} |\vec{a}_{D^*}| \\ m_{D^*} &\neq m_D, \quad d_{D^*} \neq d_D, \quad d_{D^*} = \epsilon, \quad d_D \neq \epsilon \\ (|\vec{F}_{D^*}| &= |\vec{F}_D|) \wedge (d_{D^*} \neq d_D) \Rightarrow (m_{D^*} \neq m_D), \end{aligned} \quad (47)$$

so finally we can encode the $(n = 3)$ -PPM chaotic system state of X with a total of 2-PPMs because, in addition to m_O , we've obtained the m_{D^} for $\vec{x}_{D^*} \in T^1$ with the relevant net OPS quantities!*

2. See Figure 6.

Thus, from eq. (50) in [61], we propose that the NGNBSSA's IHRE Lagrangian for m_O and m_{D^*} may be defined as

$$\mathcal{L}[m_O, \vec{x}_{D^*}, m_{D^*}, \vec{\vartheta}_{D^*}] \equiv E_K[m_{D^*}, \vec{\vartheta}_{D^*}] - E_P[m_O, \vec{x}_{D^*}] \quad (48)$$

using our generalized coordinates, where E_K and E_P are the IHRE kinetic and IHRE potential, respectively, for the IHR-PPM m_{D^*} relative to the O-PPM m_O . Using eq. (51) in [61] we define the E_P between m_O and m_{D^*} as

$$E_P[m_O, \vec{x}_{D^*}] \equiv \frac{\sqrt{1 - 2 \left(\frac{m_O}{|\vec{x}_{D^*}|} \right)}}{|\vec{x}_{D^*}|} \equiv \frac{\sqrt{1 - 2 \left(\frac{m_O}{\epsilon} \right)}}{\epsilon}, \quad (49)$$

and subsequently employ eq. (52) in [61] to define the corresponding E_K as

$$E_K[m_{D^*}, \vec{\vartheta}_{D^*}] \equiv \frac{1}{2} m_{D^*} |\vartheta_{D^*}|^2 \equiv \frac{1}{2} \left(\frac{|\vec{F}_{D^*}|}{|a_{D^*}|} \right) |\vartheta_{D^*}|^2, \quad (50)$$

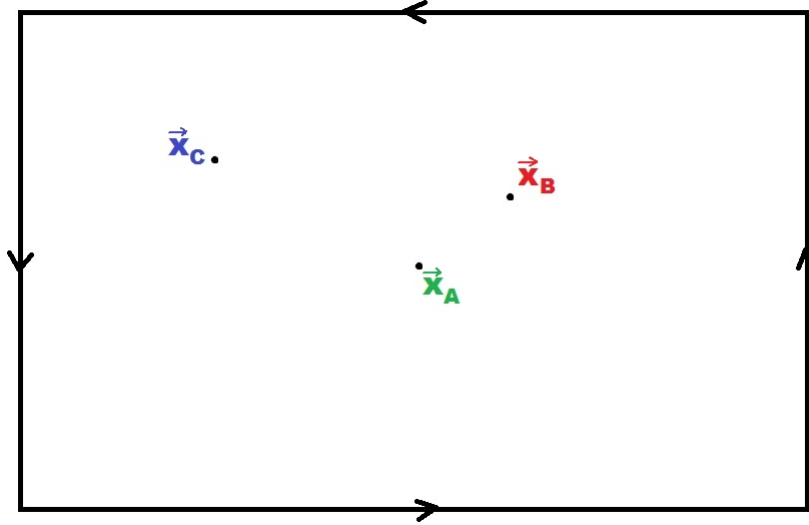


Fig. 1: The Routine 1 depiction of the $n = 3$ NGNBSSA. The three 2D-PPSs $\{\vec{x}_A, \vec{x}_B, \vec{x}_C\} = P_X \subset X$ correspond to the ordered 3-body set $\{m_A, m_B, m_C\} = M_X$.

where ϑ_{D^*} is the *IHRE RVOPS* (net value) of m_{D^*} at \vec{x}_{D^*} relative to m_O at O in the 3D IHR topology of X . Here, we note that the above NGNBSSA results and particularly eqs. (48–50) are preliminary outcomes that must be subjected to additional scrutiny in future work.

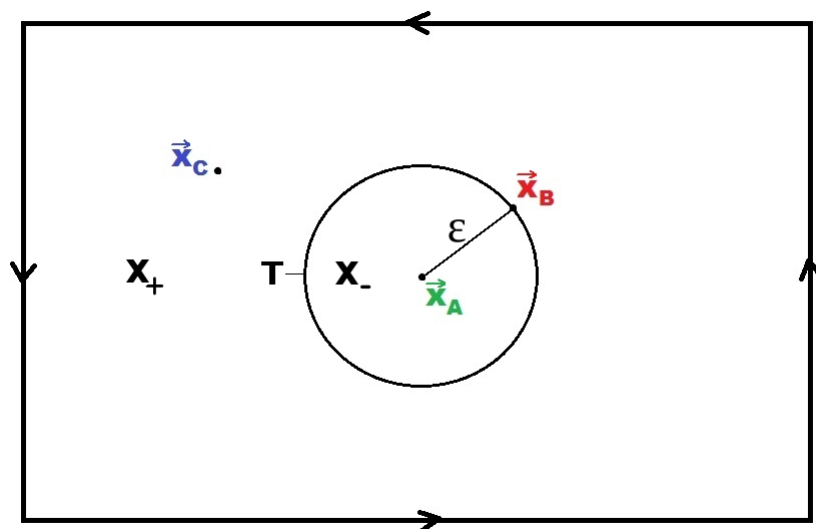


Fig. 2: The Routine 2 depiction of the $n = 3$ NGNBSSA. The 2D-PPS \vec{x}_A is the center of the 1-sphere IHR $T^1 \subset X$, which is isometrically embedded on X , where $\vec{x}_B \in T^1$.

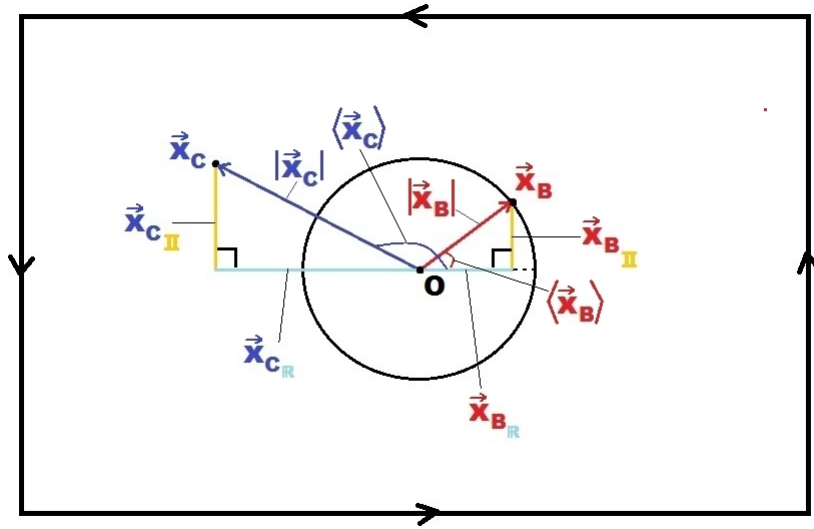


Fig. 3: The Routine 3 depiction of the $n = 3$ NGNBSSA. The 2D-PPS $O = \vec{x}_A$ becomes X 's origin for the reference frame. Using Newton's laws, we assign 2D-FOPSSs and 2D-AOPSSs to the 2D-PPMs m_B and m_C located at the 2D-PPSSs \vec{x}_B and \vec{x}_C , respectively, such that $|\vec{x}_B| = \epsilon$ and $|\vec{x}_C| \neq \epsilon$, respectively.

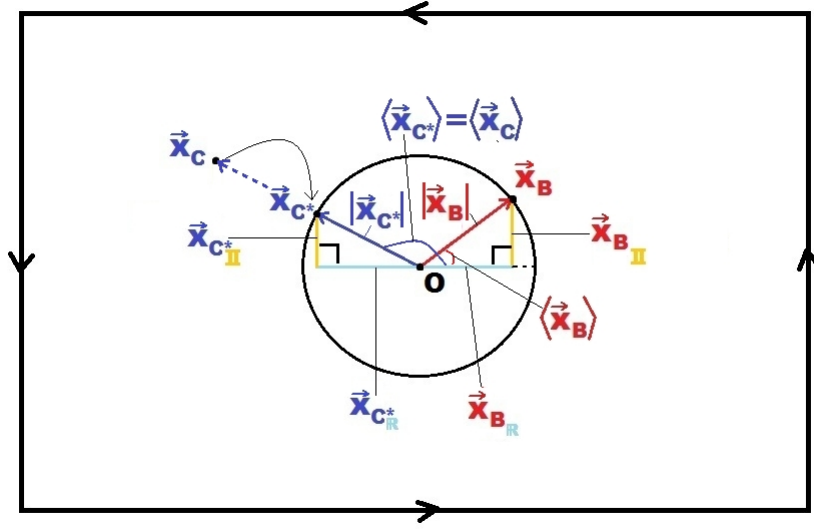


Fig. 4: The Routine 4 depiction of the $n = 3$ NGNBSSA. The objective is to IHRE-NA map all of the external 2D-PPSs in X_+ to T^1 so one 2D-PPM, namely the O-PPM m_O , is at O , while the residual $(n - 1)$ 2D-PPMs are mapped to T^1 to construct the IHRE-PPM Set, which is a foundation and prerequisite for the construction of the Initial and Final IHRE-PPM Singletons. The procedure adheres to the IHRE-NA Phase Constraint and the IHRE-NA Amplitude Constraint that enable us simplify the problem state with IHRE-NAs. Here, we have $\vec{x}_B \in T^1$, so the 2D-PPM m_B already lies precisely on T^1 . But $\vec{x}_C \in X_+$, so $\vec{x}_C \notin T^1$ is an external 2D-PPS, thus we must use X 's built-in IHR duality to deploy the IHRE-NA mapping $\vec{x}_C \rightarrow \vec{x}_{C^*}$ to create the corresponding m_{C^*} for T^1 because we need some $\vec{x}_{C^*} \in T^1$.

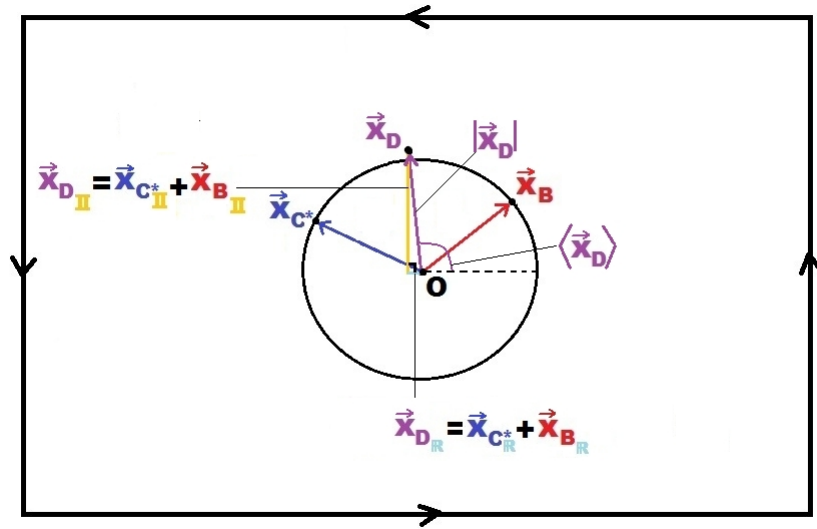


Fig. 5: The Routine 5 depiction of the $n = 3$ NGNBSSA. The *net 2D-FOPS* \vec{F}_D is the 2D-FOPS sum of \vec{F}_B and \vec{F}_{C^*} for the resulting gravitational force field that corresponds to the Initial IHRE-PPS Singleton \vec{x}_D and the Initial IHRE-PPM Singleton m_D . This consolidates the residual $(n - 1)$ 2D-PPMs to m_D to establish an IHRE 2-body system composed of m_O and m_D ; now there are just 2-bodies to deal with!

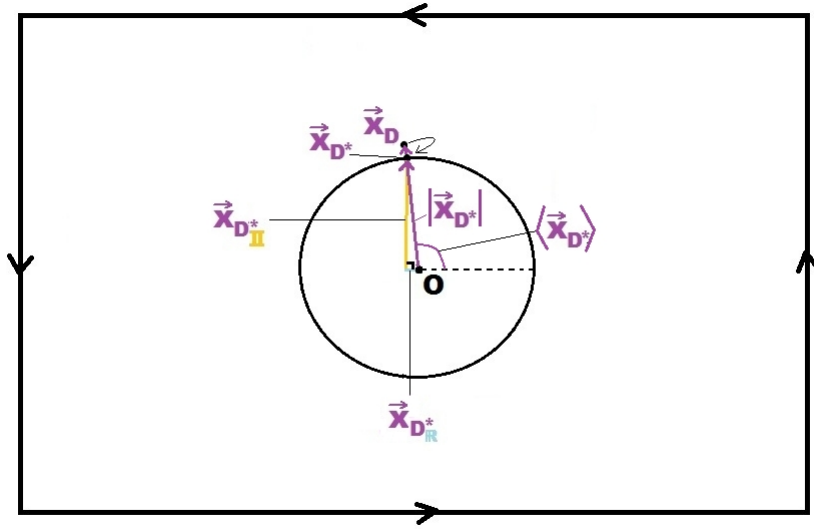


Fig. 6: The Routine 6 depiction of the $n = 3$ NGNBSSA. So $\vec{x}_D \notin T$, thus for $\vec{x}_D \in X_+$ we identify the corresponding Final IHRE-PPS Singleton $\vec{x}_{D^*} \in T$ via the IHRE-NA $\vec{x}_D \rightarrow \vec{x}_{D^*}$ to calculate the Final IHRE-PPM Singleton m_{D^*} . Now we've finally delivered a gravitationally normalized IHRE-based 2-body system of m_O and m_{D^*} !

3.2 3D algorithm for the 4D IHR topology

So how do we apply our NGNBSSA to the 4D IHR topology? Well first, we recall that in Section 2.2 we've already provided a preliminary 3D framework for encoding locations and features in the 4D IHR topology. Hence, our initial step is to revisit the NGNBSSA of Section 3.1 and simply swap the 2D data structures in Section 2.1 with their 3D counterparts in Section 2.2. Moreover, we also recall that the NGNBSSA is almost identical for both 3D and 4D IHR topology scenarios, $\forall n > 2$, but there are a couple of slight modifications that we need to make:

- ***In Routine 1:***

1. Replace the 2D-PPSS X with the 3D-PPSS Y .
2. Replace the ordered 2D-PPS set P_X of eqs. (1–2) with the ordered 3D-PPS set P_Y of eqs. (18–19).
3. Replace the ordered 2D-PPM set M_X of eq. (3) with the ordered 3D-PPM set M_Y of eq. (20).
4. Replace the ordered 2D-VOPS set V_X of eqs. (4–5) with the ordered 3D-VOPS set V_Y of eqs. (21–22).

- ***In Routine 2:***

1. Use the 3D Euclidean distance of eq. (25) instead of the 2D Euclidean distance of eq. (8).
2. Replace 2D form of T^1 from eq. (15) in [61] with the 3D form of T^2 from eq. (40) in [60].

- ***In Routine 3:***

1. Replace the 2D-FOPS notation of eq. (9) with the 3D-FOPS notation of eq. (26) and add the pertinent 3D-FOPS-inclination equivalences.
2. Replace the 2D-AOPS notation of eq. (12) with the 3D-AOPS notation of eq. (29) and add the pertinent 3D-AOPS-inclination equivalences.

3. Replace the 2D-RVOPS notation of eq. (15) with the 3D-RVOPS notation of eq. (33).

- ***In Routine 4:***

1. Create, define, and apply the IHRE-NA Inclination Constraint

$$[\vec{y}_{C^*}] = [\vec{y}_C] = [\vec{F}_{C^*}] = [\vec{F}_C] = [\vec{a}_{C^*}] = [\vec{a}_C] \quad (51)$$

to extend the IHRE-NAs to an additional degree of freedom.

- ***In Routine 5:***

1. Replace T^1 's 2D IHRE-PPM construction with a 3D IHRE-PPM construction for T^2 .

- ***In Routine 6:***

1. Apply the IHRE-NA Inclination Constraint of Routine 4 to finalize construction of T^2 's 3D IHRE-PPM.

Thus, we've listed the requisite modifications to apply the NGNBSSA to the 4D IHR topology.

At this point, we propose that the 2D IHRE Lagrangian definition of eq. (48) may be re-written in the 3D form

$$\mathcal{L}[m_O, \vec{y}_{D^*}, m_{D^*}, \vec{\vartheta}_{D^*}] \equiv E_K[m_{D^*}, \vec{\vartheta}_{D^*}] - E_P[m_O, \vec{y}_{D^*}], \quad (52)$$

so eq. (49) becomes

$$E_P[m_O, \vec{y}_{D^*}] \equiv \frac{\sqrt{1 - 2 \left(\frac{m_O}{|\vec{y}_{D^*}|} \right)}}{|\vec{y}_{D^*}|} \equiv \frac{\sqrt{1 - 2 \left(\frac{m_O}{\epsilon} \right)}}{\epsilon}, \quad (53)$$

and eq. (50) becomes

$$E_K[m_{D^*}, \vec{\vartheta}_{D^*}] \equiv \frac{1}{2} m_{D^*} |\vartheta_{D^*}|^2 \equiv \frac{1}{2} \left(\frac{|\vec{F}_{D^*}|}{|a_{D^*}|} \right) |\vartheta_{D^*}|^2 \quad (54)$$

for the 4D IHR topology of $T^2 \subset Y$.

4 Conclusion and discussion

In this preliminary paper, we introduced, defined, and constructed a framework that is designed to simplify certain aspects of Newton's gravitational n -body problem. We started by outlining the importance of further comprehending the chaos inherent to this natural problem, which applies to multiple and diverse realms within the disciplines of science, mathematics, computation, and engineering. Subsequently, we assembled the IHR topology, generalized coordinate system, and modified (superfluid) order parameter data structures to implement the first version of our NGNBSSA. During this initial pursuit, we demonstrated that the obtained results are significant because our developing NGNBSSA framework provides an abstract, powerful, and flexible state space encoding methodology for n -body chaotic gravitational systems with some possible creative applications to the said disciplines. Moreover, we found that the NGNBSSA and its structural framework encompass a relatively simplistic formulation which enables us to represent variable degrees of complexity for this mode of analysis.

For the future, we suggest that this model should be extended to include additional aspects of classical, quantum, and relativistic mechanics for physics, chaos, and fractal geometry via the scientific method. It may be intriguing and beneficial to implement the NGNBSSA on a super-computing cluster so one can conduct parallel simulations to further refine the direct practicality of these ideas. Also, it may be beneficial to match the predictions of this theory with, for example, real-time astronomical data and conduct high-energy physics experiments to prove (or disprove) pertinence to hadronic mechanics [64, 65] and magnecoles [66, 67, 68, 69, 70, 71, 72]. Furthermore, an iso-mathematics [73, 74, 75, 76, 77] treatment for the NGNBSSA should be in order.

In our opinion, the NGNBSSA is a powerful systematic process with an *enormous* potential for direct application to modern physics—theoretical *and* experimental. So although this model is still under development, we suspect that through further investigation, scrutiny, refinement, collaboration, and hard work, these ideas may reveal additional key facets in mathematics, computation, engineering, and science.

5 Acknowledgment

I wish to thank the anonymous referees for the useful comments and constructive criticism that helped me upgrade the content of this paper.

References

- [1] B. M. Gessen and J. Herivel. *The background to Newton's Principia: a study of Newton's dynamical researches in the years 1664-84*. Clarendon Press, 1965.
- [2] I. Newton. *Principia, vol. I: the motion of bodies*. University of California Press, 1966.
- [3] K. Huang and C. N. Yang. Quantum-mechanical many-body problem with hard-sphere interaction. *Physical review*, 105(3):767, 1957.
- [4] T. D. Lee and C. N. Yang. Many-body problem in quantum mechanics and quantum statistical mechanics. *Physical Review*, 105(3):1119, 1957.
- [5] F. E. Udadia and R. E. Kalaba. *Analytical dynamics: a new approach*. Cambridge University Press, 2007.
- [6] N. H. March, W. H. Young, and S. Sampanthar. *The many-body problem in quantum mechanics*. Courier Dover Publications, 1967.
- [7] A. D. Bruno. *The restricted 3-body problem: plane periodic orbits*, volume 17. de Gruyter, 1994.
- [8] S. H. Kellert. *In the wake of chaos: Unpredictable order in dynamical systems*. University of Chicago Press, 1993.
- [9] E. N. Lorenz. *The essence of chaos*. Routledge, 1995.
- [10] G. W. Flake. *The computational beauty of nature: Computer explorations of fractals, chaos, complex systems and adaption*. The MIT Press, 1998.
- [11] J. Briggs. *Fractals: The patterns of chaos: A new aesthetic of art, science, and nature*. Touchstone Books, 1992.
- [12] B. B. Mandelbrot. *The fractal geometry of nature*. Times Books, 1982.
- [13] I. Stewart. *Does God play dice?: The new mathematics of chaos*. Penguin UK, 1997.
- [14] H. Nagashima and Y. Baba. *Introduction to chaos: physics and mathematics of chaotic phenomena*. CRC Press, 2002.
- [15] L. Bombelli and E. Calzetta. Chaos around a black hole. *Classical and Quantum Gravity*, 9(12):2573–2599, 1992.

- [16] M. S. El Naschie. Fractal black holes and information. *Chaos, Solitons & Fractals*, 29(1):23–35, 2006.
- [17] S. H. Strogatz. *Nonlinear dynamics and chaos: with applications to physics, biology and chemistry*. Perseus publishing, 2001.
- [18] X. Wu and T. Huang. Computation of lyapunov exponents in general relativity. *Physics Letters A*, 313(1):77–81, 2003.
- [19] L. B. Crowell and C. Corda. (r) gravity, relic coherent gravitons and optical chaos. *Galaxies*, 2(1):160–188, 2014.
- [20] J. Gaite and S. C. Manrubia. Scaling of voids and fractality in the galaxy distribution. *Monthly Notices of the Royal Astronomical Society*, 335(4):977–983, 2002.
- [21] N. Sánchez and E. J. Alfaro. The fractal distribution of h ii regions in disk galaxies. *The Astrophysical Journal Supplement Series*, 178(1):1–19, 2008.
- [22] B. Peng, V. Petrov, and K. Showalter. Controlling chemical chaos. *The Journal of Physical Chemistry*, 95(13):4957–4959, 1991.
- [23] R. J. Field and L. Györgyi. *Chaos in chemistry and biochemistry*. World Scientific, 1993.
- [24] P. W. O. Hoskin. Patterns of chaos: fractal statistics and the oscillatory chemistry of zircon. *Geochimica et Cosmochimica Acta*, 64(11):1905–1923, 2000.
- [25] P. Philippe. Chaos, population biology, and epidemiology: some research implications. *Human Biology*, 65(4):525, 1993.
- [26] L. Bos and et al. *Plant viruses, unique and intriguing pathogens: a textbook of plant virology*. Backhuys Publishers, 1999.
- [27] P. Duesberg. Chromosomal chaos and cancer. *Scientific American Magazine*, 296(5):52–59, 2007.
- [28] G. B. West, J. H. Brown, and B. J. Enquist. A general model for the origin of allometric scaling laws in biology. *Science*, 276(5309):122–126, 1997.
- [29] G. B. West, J. H. Brown, and B. J. Enquist. The fourth dimension of life: fractal geometry and allometric scaling of organisms. *Science*, 284(5420):1677–1679, 1999.
- [30] R. Wu, C. X. Ma, R. C. Littell, and G. Casella. A statistical model for the genetic origin of allometric scaling laws in biology. *Journal of*

- theoretical biology*, 219(1):121–135, 2002.
- [31] G. B. West and J. H. Brown. The origin of allometric scaling laws in biology from genomes to ecosystems: towards a quantitative unifying theory of biological structure and organization. *Journal of Experimental Biology*, 208(9):1575–1592, 2005.
 - [32] L. Demetrius. The origin of allometric scaling laws in biology. *Journal of theoretical biology*, 243(4):455–467, 2006.
 - [33] C. A. Skarda and W. J. Freeman. Chaos and the new science of the brain. *Concepts in Neuroscience*, 1(2):275–285, 1990.
 - [34] S. J. Schiff, K. Jerger, D. H. Duong, T. Chang, M. L. Spano, William L. Ditto, and et al. Controlling chaos in the brain. *Nature*, 370(6491):615–620, 1994.
 - [35] H. Haken. *Principles of brain functioning: A synergetic approach to brain activity, behavior and cognition*. Springer Publishing Company, Incorporated, 2012.
 - [36] D. S. Coffey. Self-organization, complexity and chaos: the new biology for medicine. *Nature medicine*, 4(8):882–885, 1998.
 - [37] B. J. West. *Fractal physiology and chaos in medicine*, volume 16. World Scientific, 2013.
 - [38] J. P. Crutchfield and K. Young. Computation at the onset of chaos. In *The Santa Fe Institute, Westview*. Citeseer, 1988.
 - [39] R. L. Devaney. *Chaos and fractals: The mathematics behind the computer graphics*. American Mathematical Soc., 1989.
 - [40] N. Bertschinger and T. Natschläger. Real-time computation at the edge of chaos in recurrent neural networks. *Neural computation*, 16(7):1413–1436, 2004.
 - [41] L. Kocarev. Chaos-based cryptography: a brief overview. *Circuits and Systems Magazine, IEEE*, 1(3):6–21, 2001.
 - [42] G. Jakimoski, L. Kocarev, and et. al. Chaos and cryptography: block encryption ciphers based on chaotic maps. *IEEE Transactions on Circuits and Systems I: Fundamental Theory and Applications*, 48(2):163–169, 2001.
 - [43] M. A. Alia and A. Samsudin. A new digital signature scheme based on mandelbrot and julia fractal sets. *American Journal of Applied Sciences*, 4(11):850–858, 2007.

- [44] B. LeBaron. Chaos and nonlinear forecastability in economics and finance. *Philosophical Transactions of the Royal Society of London. Series A: Physical and Engineering Sciences*, 348(1688):397–404, 1994.
- [45] J. B. Rosser. *From Catastrophe to Chaos: A General Theory of Economic Discontinuities: Mathematics, Microeconomics and Finance*, volume 1. Springer, 2000.
- [46] D. Nicholls, T. Tagarev, and P. Axup. What does chaos theory mean for warfare. *Airpower Journal*, pages 48–57, 1994.
- [47] G. E. James. *Chaos Theory: The Essentials for Military Applications*. Number 10. Naval War College, Center for Naval Warfare Studies, 1996.
- [48] A. Bousquet. *The scientific way of warfare: Order and chaos on the battlefields of modernity*, volume 1. Cinco Puntos Press, 2009.
- [49] J. Gleick. Chaos: Making a new science. 2008.
- [50] J. Huisman and F. J. Weissing. Biodiversity of plankton by species oscillations and chaos. *Nature*, 402(6760):407–410, 1999.
- [51] A. A. Tsonis and J. B. Elsner. Chaos, strange attractors, and weather. *Bulletin of the American Meteorological Society*, 70:14–23, 1989.
- [52] G. A. Calin, C. Vasilescu, M. Negrini, and G. Barbanti-Brodano. Genetic chaos and antichaos in human cancers. *Medical hypotheses*, 60(2):258–262, 2003.
- [53] S. L. Harris. *Agents of chaos: earthquakes, volcanoes, and other natural disasters*. Mountain Press Publishing Company, 1990.
- [54] H. J. Xu and L. Knopoff. Periodicity and chaos in a one-dimensional dynamical model of earthquakes. *Physical Review E*, 50(5):3577, 1994.
- [55] C. H. Scholz. Earthquakes as chaos. *Nature*, 348(6298):197–198, 1990.
- [56] D. Larsen-Freeman. Chaos/complexity science and second language acquisition. *Applied linguistics*, 18(2):141–165, 1997.
- [57] H. O. Peitgen, H. Jürgens, and D. Saupe. *Chaos and fractals: new frontiers of science*. Springer, 2004.
- [58] M. R. Schroeder. *Fractals, chaos, power laws: Minutes from an infinite paradise*. Courier Dover Publications, 2012.
- [59] B. B. Mandelbrot. *Fractals and chaos: the Mandelbrot set and beyond*, volume 3. Springer, 2004.
- [60] N. O. Schmidt. A complex and triplex framework for encoding the Riemannian dual space-time topology equipped with order parameter

- fields. *The Hadronic Journal*, 35(6):671, 2012.
- [61] A. E. Inopin and N. O. Schmidt. Proof of quark confinement and baryon-antibaryon duality: I: Gauge symmetry breaking in dual 4D fractional quantum Hall superfluidic space-time. *The Hadronic Journal*, 35(5):469, 2012.
- [62] A. J. Leggett. A theoretical description of the new phases of liquid He 3. *Reviews of Modern Physics*, 47(2):331, 1975.
- [63] L. Susskind. The world as a hologram. *Journal of Mathematical Physics*, 36(11):6377–6396, 1995.
- [64] R. M. Santilli. *Elements of hadronic mechanics*, volume 3. Naukova Dumka, 1995.
- [65] R. M. Santilli. Hadronic mathematics, mechanics and chemistry. *Volumes I, II, III, IV and V, International Academic Press*, 2008.
- [66] R. M. Santilli. Theoretical prediction and experimental verifications of the new chemical species of magnequles. *Hadronic Journal*, 21:789–894, 1998.
- [67] I. Gandzha and J. V. Kadeisvili. New sciences for a new era: Mathematical, physical and chemical discoveries of Ruggero Maria Santilli, 2011.
- [68] R. M. Santilli and D. D. Shillady. A new iso-chemical model of the hydrogen molecule. *International Journal of Hydrogen Energy*, 24(10):943–956, 1999.
- [69] R. M. Santilli. The new chemical species of magnequles. *Foundations of Hadronic Chemistry*, pages 303–389, 2002.
- [70] Y. Yang, J. V. Kadeisvili, and S. Marton. Additional experimental confirmations of the new chemical species of Santilli magnequles. *Open Physical Chemistry Journal*, 7(1), 2013.
- [71] R. M. Santilli. Experimental detections of h_3o , coh , co_2h , and other anomalous species. 2013.
- [72] R. Brenna, T. Kuliczowski, and L. Ying. Verification of intermediate nuclear fusions without harmful radiation and the production of magnequclular clusters. *New Advances in Physics*, 5(1), 2011.
- [73] R. M. Santilli. Isonumbers and genonumbers of dimensions 1, 2, 4, 8, their isoduals and pseudoduals, and "hidden numbers" of dimension 3, 5, 6, 7. *Algebras, Groups and Geometries*, 10:273, 1993.

- [74] R. M. Santilli. Rendiconti circolo matematico di palermo. *Supplemento*, 42:7, 1996.
- [75] C. X. Jiang. Fundaments of the theory of Santillian numbers. *International Academic Presss, America-Europe-Asia*, 2002.
- [76] C. Corda. Introduction to Santilli iso-numbers. In *AIP Conference Proceedings-American Institute of Physics*, volume 1479, page 1013, 2012.
- [77] C. Corda. Introduction to Santilli iso-mathematics. In *AIP Conference Proceedings-American Institute of Physics*, volume 1558, page 685, 2013.